A&A 435, 1191–1198 (2005)
DOI: 10.1051/0004-6361:20042318
© ESO 2005

Astronomy & Astrophysics

On the influence of Stark broadening on Cr I lines in stellar atmospheres

M. S. Dimitrijević[1,2], T. Ryabchikova[3,4], L. Č. Popović[1,2,5], D. Shulyak[6], and S. Khan[6]

[1] Astronomical Observatory, Volgina 7, 11160 Belgrade 74, Serbia
[2] Isaac Newton Institute of Chile, Yugoslavia Branch, Yugoslavia
e-mail: mdimitrijevic@aob.bg.ac.yu
[3] Institute of Astronomy, Russian Academy of Science, Pyatnitskaya 48, 119017 Moscow, Russia
[4] Institute for Astronomy, University of Vienna, Türkenschanzstrasse 17, 1180 Vienna, Austria
[5] Astrophysikalisches Institut Potsdam, An der Sternwarte 16, 14482 Potsdam, Germany
[6] Tavrian National University, Yaltinskaya 4, 330000 Simferopol, Crimea, Ukraine

Received 5 November 2004 / Accepted 17 January 2005

Abstract. Using the semiclassical perturbation method, electron-, proton-, and ionized helium-impact line widths and shifts for the nine Cr I spectral lines from the $4p^7P^0-4d^7D$ multiplet were calculated for a perturber density of 10^{14} cm^{-3} and for temperatures T = 2500−50 000 K. The results were used to investigate the influence of Stark broadening effect in the Cr-rich Ap star β CrB atmosphere on line shapes of these lines. It was found that the contribution of proton and He II collisions to the line width and shift is significant and comparable, and is sometimes even larger than electron-impact contribution depending of the electron temperature. Moreover, not only the Stark line width, but also the Stark shift may contribute to the blue as well as to the red asymmetry of the same line depending on the electron-, proton-, and He II density in stellar atmosphere. The results were used to investigate the influence of Stark broadening effect on Cr I line shapes in the atmosphere of the Cr-rich Ap star β CrB.

Key words. atomic processes – line: profiles – stars: chemically peculiar – stars: individual: β CrB

1. Introduction

Stark broadening is the most significant pressure broadening mechanism for A and B stars, such that this effect should be taken into account in investigation, analysis, and modelling of their atmospheres. In our previous works (Popović et al. 1999, 2001; Dimitrijević et al. 2003) we have shown that Stark broadening may change spectral line equivalent widths by 10−45%; hence neglecting this mechanism may introduce significant errors in abundance determinations. Stark data become extremely important after discovering abundance gradients in the atmospheres of magnetic, chemically peculiar (Ap) stars (Babel 1992; Ryabchikova et al. 2002; Wade et al. 2003). High resolution spectra allow us to perform stratification analysis using line profiles, and strong lines with developed wings provide us with the most accurate information about distribution of the element through the stellar atmosphere (see Dimitrijević et al. 2003 for Si).

Chromium is one of the most anomalous elements in Ap stars. It was shown to be concentrated in the deeper atmospheric layers in Ap stars β CrB (Wade et al. 2003) and in γ Equ (Ryabchikova et al. 2002), where electron density is high enough to favor the Stark effect. Most Cr I and Cr II lines in the optical spectral region have rather small Stark damping constants so no measurable Stark wings appeared. However, Cr I lines from 4p−4d transitions are known to have fairly large Stark damping constants according to calculations made by Kurucz (1993).

We present new calculations of Cr I line Stark widths and shifts based on the semiclassical perturbation approach (Sahal-Bréchot 1969a,b, 1974; Dimitrijević & Sahal-Bréchot 1984a). Calculation method is described in Sect. 2 and magnetic synthetic spectrum calculations are described in Sect. 3. Results of Stark broadening calculations are given in Sect. 4.1, while an application of new data to spectrum synthesis in magnetic Ap star β CrB is considered in Sect. 4.2.

2. The Stark broadening parameter calculation

Calculations have been performed within the semiclassical perturbation formalism, as developed and discussed in detail in Sahal-Bréchot (1969a,b). This formalism, as well as the corresponding computer code, have been optimized and updated several times (see e.g. Sahal-Bréchot 1974; Dimitrijević & Sahal-Bréchot 1984a; Dimitrijević 1996).

Within this formalism, the full width of a neutral emitter isolated spectral line broadened by electron impacts can be

Article published by EDP Sciences and available at http://www.edpsciences.org/aa or http://dx.doi.org/10.1051/0004-6361:20042318

expressed in terms of cross sections for elastic and inelastic processes as

$$W_{if} = \frac{2\lambda_{if}^2}{2\pi c} n_{\rm e} \int v f(v) {\rm d}v \left(\sum_{i' \neq i} \sigma_{ii'}(v) + \sum_{f' \neq f} \sigma_{ff'}(v) + \sigma_{\rm el} \right) \quad (1)$$

and the corresponding line shift as

$$d_{if} = \frac{\lambda_{if}^2}{2\pi c} n_{\rm e} \int v f(v) {\rm d}v \int_{R_3}^{R_D} 2\pi\rho {\rm d}\rho \sin 2\phi_{\rm p}. \quad (2)$$

Here, λ_{if} is the wavelength of the line originating from the transition with the initial atomic energy level i and the final level f; c is the velocity of light; $n_{\rm e}$ the electron density; $f(v)$ the Maxwellian velocity distribution function for electrons; m the electron mass; k the Boltzmann constant; T the temperature, and ρ denotes the impact parameter of the incoming electron. The inelastic cross section $\sigma_{jj'}(v)$ is determined according to Chap. 3 in Sahal-Bréchot (1969b) and elastic cross section $\sigma_{\rm el}$ according to Sahal-Bréchot (1969a). The cut-offs, included in order to maintain unitarity of the S-matrix, are described in Sect. 1 of Chap. 3 in Sahal-Bréchot (1969a).

The formulae for the ion-impact broadening parameters are analogous to the formulae for electron-impact broadening. For the colliding ions, the validity of the impact approximation has to be checked in the far wings.

3. Line profile calculations

Model atmosphere calculations, as well as calculations of the absorption coefficients, were made with the local thermodynamical equilibrium (LTE) approximation. Model calculations were performed with the ATLAS9 code (Kurucz 1993), modified by Piskunov & Kupka (2001) to include individual chemical composition of the star in line opacity calculations (see Kupka et al. 2004).

The next step is to calculate the outward flux at corresponding wavelength points using the given model. For this purpose we used SYNTHM code written by Khan (2004). This code allows synthetic spectra of early and intermediate type of stars to be calculated taking magnetic field effects into account along with stratification of chemical elements.

The computational scheme is as follows. For each line we find the central opacity as

$$\alpha_{\rm line} = \frac{\pi e^2}{mc} g f_{if} {\rm e}^{-\frac{\chi}{kT}} \frac{n}{\rho} \left(1 - {\rm e}^{-\frac{h\nu}{kT}}\right), \quad (3)$$

where α_ν is the mass absorption coefficient at frequency ν; e the electron charge; g the statistical weight; f_{if} the oscillator strength for a given transition; χ the excitation energy; n the number density of a corresponding element in a given ionization stage multiplied by partition function; ρ the density and h the Planck constant. The last factor describes stimulated emission.

Next, we compute the total damping parameter

$$\gamma = \gamma_{\rm rad} + \gamma_{\rm Stark} + \gamma_{\rm neutral}. \quad (4)$$

Here $\gamma_{\rm rad}$, $\gamma_{\rm Stark}$, and $\gamma_{\rm neutral}$ are the radiative broadening, Stark broadening, and damping parameters due to neutral atom collisions, respectively. The values of $\gamma_{\rm rad}$, $\gamma_{\rm neutral}$, excitation energy χ and oscillator strength gf were taken from the Vienna Atomic Line Database (VALD) (Kupka et al. 1999). In the case of neutral atom broadening we assumed that perturbing particles are only neutral hydrogen and helium atoms (Van der Waals broadening). This assumption is applicable to almost all types of stars due to high hydrogen and helium cosmic abundances. We shall discuss competition between the broadenings caused by the Stark effect and by neutral hydrogen collisions in the atmospheres of our template star β CrB in Sect. 4.2.

In order to take into account Stark broadening effects we added the approximate formulas Eqs. (20) and (21) (Sect. 4.1) to the code. The Stark width and shift are

$$\gamma_{\rm Stark} = \gamma_{\rm Stark}^{\rm (e)} n_{\rm e} + \gamma_{\rm Stark}^{\rm (p)} n_{\rm p} + \gamma_{\rm Stark}^{\rm (HeII)} n_{\rm HeII}, \quad (5)$$

$$d_{\rm Stark} = d_{\rm Stark}^{\rm (e)} n_{\rm e} + d_{\rm Stark}^{\rm (p)} n_{\rm p} + d_{\rm Stark}^{\rm (HeII)} n_{\rm HeII}, \quad (6)$$

where $n_{\rm e}$, $n_{\rm p}$ and $n_{\rm HeII}$ are the corresponding densities of electrons, protons, and He II ions respectively. The resulting opacity profile is given by the Voigt function (Doppler + pressure broadening).

The next step is to solve the transfer equation with new Stark damping parameters. In the presence of magnetic field, atomic level k determined by quantum numbers J_k, L_k, S_k splits into $2J_k + 1$ states with $M_k = -J_k, \ldots, +J_k$. The absolute value of splitting is defined by field modulus $|\boldsymbol{B}|$ and Landé factor g_k, which in the case of LS coupling is calculated as

$$g_k = \frac{3}{2} + \frac{S_k(S_k+1) - L_k(L_k+1)}{2J_k(J_k+1)}. \quad (7)$$

The possible transitions between split levels (u – upper and l – lower level) are allowed by selection rules

$$\Delta M = M_u - M_l = \begin{cases} +1 \equiv b, \\ 0 \equiv p, \\ -1 \equiv r. \end{cases} \quad (8)$$

For a normal Zeeman triplet the subscript p corresponds to the unshifted π component, whereas b and r correspond to the blue- and red-shifted σ components, respectively. In the general case of an anomalous splitting, indices p, b, r refer to the series of the π and σ components.

The wavelength shift of the component relative to the laboratory line centre λ_0 is defined by

$$\Delta\lambda = \frac{e\lambda_0^2 |\boldsymbol{B}|}{4\pi mc^2} \left(g_l M_l - g_u M_u\right). \quad (9)$$

The relative strengths of components $S_{p,r,b}$ in accordance with Sobelman (1977) are proportional to

$$\begin{pmatrix} J_u & 1 & J_l \\ -M_u & (M_u - M_l) & M_l \end{pmatrix}^2, \quad (10)$$

where the last structure is a $3j$-symbol. The normalization of components is done so that

$$\sum S_p = \sum S_b = \sum S_r = 1. \quad (11)$$

Article published by EDP Sciences and available at http://www.edpsciences.org/aa or http://dx.doi.org/10.1051/0004-6361:20042318

In a general case the polarized radiation can be described by means of Stokes $IQUV$ parameters. The transfer equation is

$$\frac{\mathrm{d}\boldsymbol{I}}{\mathrm{d}z} = -\boldsymbol{K}\boldsymbol{I} + \boldsymbol{J}. \tag{12}$$

Here $\boldsymbol{I} = (I, Q, U, V)^T$ is the Stokes vector, $\boldsymbol{K}$ the absorption matrix and $\boldsymbol{J}$ the emission vector,

$$\boldsymbol{K} = \alpha_\mathrm{c}\mathbf{1} + \sum_{\mathrm{lines}} \alpha_\mathrm{line}\boldsymbol{\Phi}_\mathrm{line}, \tag{13}$$

$$\boldsymbol{J}_\nu = \alpha_\mathrm{c} B_\nu(T)\boldsymbol{e_0} + B_\nu(T)\sum_{\mathrm{lines}} \alpha_\mathrm{line}\boldsymbol{\Phi}_\mathrm{line}\boldsymbol{e_0}, \tag{14}$$

where $\mathbf{1}$ is the 4×4 unit matrix, $\boldsymbol{e_0} = (1,0,0,0)^T$, α_c the continuum absorption coefficient, α_line the line central opacity for zero damping and the zero magnetic field given by Eq. (3). Here we also assume LTE, so that the source function is equal to Planck function $B_\nu(T)$.

The line absorption matrix $\boldsymbol{\Phi}_\mathrm{line}$ is created with absorption profiles ϕ_j and anomalous dispersion profiles ψ_j of π and of $\sigma_\pm$ components in accordance with Rees et al. (1989). These profiles are calculated as (for $j = p, b, r$)

$$\phi_j = \sum_{i_j=1}^{N_j} S_{i_j} H\left(a, \upsilon - \frac{\Delta\lambda_{i_j}}{\Delta\lambda_\mathrm{D}}\right), \tag{15}$$

$$\psi_j = 2\sum_{i_j=1}^{N_j} S_{i_j} F\left(a, \upsilon - \frac{\Delta\lambda_{i_j}}{\Delta\lambda_\mathrm{D}}\right), \tag{16}$$

where $H(a,u)$ and $F(a,u)$ are the Voigt and Faraday-Voigt functions,

$$a = \frac{\gamma\lambda_0^2}{4\pi c\,\Delta\lambda_\mathrm{D}}, \tag{17}$$

$$\upsilon = \frac{\lambda - \lambda_0 + d_\mathrm{Stark}}{\Delta\lambda_\mathrm{D}}. \tag{18}$$

The Stark shift d_Stark and the damping parameter γ have been calculated from Eqs. (6) and (4), respectively. The Doppler width $\Delta\lambda_\mathrm{D}$ is

$$\Delta\lambda_\mathrm{D} = \frac{\lambda}{c}\sqrt{\frac{2kT}{m_\mathrm{A}} + \xi_\mathrm{t}^2}, \tag{19}$$

where m_A is the mass of the absorber atom and ξ_t the microturbulent velocity.

The transfer equation Eq. (12) is solved by the DELO method (Rees et al. 1989) with quadratic approximation for the source function, suggested by Socas-Navarro et al. (2000) and written in Fortran by Piskunov & Kochukhov (2000). Also, we used the fast Humlicek (1982) algorithm for approximations of the Voigt and Faraday-Voigt functions.

Convolution of the synthetic spectra due to stellar rotation was produced by IDL procedure of Valenti & Anderson implemented in the ROTATE IDL code by N. Piskunov.

4. Results

4.1. Stark broadening data

The atomic energy levels needed for Stark broadening calculations were taken from Wiese & Musgrove (1989). Oscillator strengths were calculated using the method of Bates & Damgaard (1949) and tables in Oertel & Shomo (1968). For higher levels, the method described in van Regemorter et al. (1979) was applied.

The neutral chromium spectrum is complex and not known well enough for a good calculation of the line being considered. The principal problem is the absence of reliable experimental data for f levels. However, by inspecting theoretically predicted Cr I levels in Moore (1971), one can see that the 4f level is missing. In accordance with the decrease in distance between existing s, p, and d levels, we estimated that the eventual 5f level should be around 52 000 cm^{-1} and not closer than 50 000 cm^{-1}. We checked results without 5f level and with a fictive 5f level at 52 000 and 50 000 cm^{-1}. In all cases, line widths differed by less than 1%, while the shift varies by several percents, so we performed calculations without the contribution of f energy levels. Since the average estimated error of the semiclassical method is ±30%, due to additional approximations and uncertainties, we estimate the error bars of our results to be ±50%.

Our results for electron-, proton-, and ionized helium-impact line widths and shifts for the nine Cr I spectral lines for a perturbed density of 10^{14} cm^{-3} and temperatures T = 2500−50 000 K are all shown in Table 1. For perturber densities lower than those tabulated here, Stark broadening parameters vary linearly with perturber density. The nonlinear behavior of Stark broadening parameters at higher densities is the consequence of the influence of Debye shielding, which has been analyzed in detail in Dimitrijević & Sahal-Bréchot (1984b).

After testing the density dependence of Stark parameters, we found that the width and shift are linear functions of density for perturber densities smaller than 10^{16} cm^{-3}. They can be scaled by the simple formula

$$(W,d)_N = (W,d)_0\left(\frac{N}{10^{14}}\right), \tag{20}$$

where $(W,d)_N$ are the width and shift at a perturber density N (cm^{-3}) and $(W,d)_0$ are width and shift given in Table 1, respectively.

In order to simplify the input of Stark broadening data in the codes for stellar spectral synthesis, we developed an analytical expression for Stark widths and shifts

$$\frac{W}{n_\mathrm{e}}\left[\text{Å}\right] = c_1\cdot\left(A + T^B\right), \tag{21}$$

$$\frac{d}{n_\mathrm{e}}\left[\text{Å}\right] = c_2\cdot\left(A + C\cdot T^B\right). \tag{22}$$

The constants c_1, c_2, A, B, and C are given in Table 2. We take T as $T/(10\,000\ \mathrm{K})$. As one can see from the analytical fit in Figs. 1 and 2, Eqs. (21) and (22) fit the calculated values in both Stark widths and shifts. In some lines here (as e.g. in Cr I λ = 5329.14 Å), the analytical fit in the case of proton

Article published by EDP Sciences and available at http://www.edpsciences.org/aa or http://dx.doi.org/10.1051/0004-6361:20042318

Table 1. Stark broadening parameters for Cr I 4p–4d spectral lines. This table shows electron-, proton-, and ionized helium-impact broadening parameters for Cr I for a perturber density of 10^{14} cm^{-3} and temperatures from 2500 up to 50 000 K. Quantity C is given in Å cm^{-3} and divided by the corresponding full width at half maximum (*FWHM*), gives an estimate for the maximum perturber density for which tabulated data may be used. The asterisk identifies cases for which the collision volume multiplied by the perturber density lies between 0.1 and 0.5. When it is larger than 0.5 results are omitted.

PERTURBERS ARE:		ELECTRONS		PROTONS		HELIUM IONS	
TRANSITION	T(K)	*FWHM*(A)	SHIFT(A)	*FWHM*(A)	SHIFT(A)	*FWHM*(A)	SHIFT(A)
Cr I $^7P^0_2$–$^7D_1$	2500.	0.890E–02	–0.205E–02	0.461E–02	–0.379E–02	0.344E–02	–0.299E–02
	5000.	0.772E–02	–0.146E–02	0.551E–02	–0.437E–02	0.388E–02	–0.346E–02
5276.07 A	10 000.	0.655E–02	–0.104E–02	0.678E–02	–0.505E–02	0.439E–02	–0.396E–02
C = 0.43E+15	20 000.	0.548E–02	–0.767E–03	0.832E–02	–0.592E–02	0.503E–02	–0.451E–02
	30 000.	0.493E–02	–0.660E–03	0.915E–02	–0.651E–02	0.547E–02	–0.488E–02
	50 000.	0.431E–02	–0.559E–03	0.993E–02	–0.719E–02	0.602E–02	–0.544E–02
Cr I $^7P^0_2$–$^7D_2$	2500.	0.193E–01	–0.216E–02				
	5000.	0.164E–01	–0.155E–02				
5275.75 A	10 000.	0.136E–01	–0.108E–02				
C = 0.11E+14	20 000.	0.111E–01	–0.790E–03	*0.717E–01	–0.298E–01		
	30 000.	0.983E–02	–0.675E–03	*0.702E–01	–0.273E–01		
	50 000.	0.841E–02	–0.569E–03	*0.664E–01	–0.239E–01	*0.135E–01	–0.346E–01
Cr I $^7P^0_2$–$^7D_3$	2500.	0.240E–01	–0.939E–03	*0.216E–01	–0.138E–01	*0.131E–01	–0.102E–01
	5000.	0.210E–01	–0.677E–03	*0.253E–01	–0.170E–01	*0.151E–01	–0.124E–01
5275.28 A	10 000.	0.178E–01	–0.473E–03	*0.274E–01	–0.193E–01	*0.169E–01	–0.150E–01
C = 0.60E+14	20 000.	0.147E–01	–0.401E–03	0.280E–01	–0.193E–01	*0.170E–01	–0.179E–01
	30 000.	0.131E–01	–0.393E–03	0.283E–01	–0.180E–01	*0.157E–01	–0.193E–01
	50 000.	0.112E–01	–0.393E–03	0.289E–01	–0.155E–01	*0.127E–01	–0.200E–01
Cr I $^7P^0_3$–$^7D_2$	2500.	0.195E–01	–0.219E–02				
	5000.	0.165E–01	–0.156E–02				
5298.49 A	10 000.	0.137E–01	–0.109E–02				
C = 0.12E+14	20 000.	0.112E–01	–0.801E–03	*0.723E–01	–0.301E–01		
	30 000.	0.992E–02	–0.685E–03	*0.708E–01	–0.276E–01		
	50 000.	0.849E–02	–0.578E–03	*0.670E–01	–0.242E–01	*0.136E–01	–0.349E–01
Cr I $^7P^0_3$–$^7D_3$	2500.	0.243E–01	–0.950E–03	*0.218E–01	–0.140E–01	*0.133E–01	–0.103E–01
	5000.	0.212E–01	–0.687E–03	*0.256E–01	–0.171E–01	*0.153E–01	–0.125E–01
5298.02 A	10 000.	0.179E–01	–0.481E–03	*0.276E–01	–0.195E–01	*0.171E–01	–0.151E–01
C = 0.60E+14	20 000.	0.148E–01	–0.408E–03	0.283E–01	–0.195E–01	*0.171E–01	–0.180E–01
	30 000.	0.132E–01	–0.400E–03	0.286E–01	–0.182E–01	*0.158E–01	–0.195E–01
	50 000.	0.113E–01	–0.400E–03	0.291E–01	–0.157E–01	*0.128E–01	–0.201E–01

and He II impact broadening parameters does not exactly fit the calculated values (see e.g. Fig. 2, with a fit for proton-impact shift), but the differences are smaller than the expected error of our calculations (≈±50%).

4.2. The Stark broadening effect on the shape of Cr I lines

In spite of the rather large Stark damping constants, the effect is not observable in stars with solar Cr abundance. In hot stars where electron and proton densities are high, the Cr I lines considered here are generally very weak, while in cooler stars (solar type) other broadening effects are more significant where these lines are strong enough. The only chance to look at Stark effect is in stratified atmosphere of a Cr-rich Ap star, such as the well known magnetic star β CrB.

Our spectral analysis was based on the β CrB spectrum obtained in February 1998 with the MuSiCoS spectropolarimeter mounted on the 2 m telescope at Pic du Midi observatory (R = 35 000). This spectrum was used by Wade et al. (2001, 2003) in stratification analysis. Starting Cr and Fe distributions were taken from this analysis and were slightly corrected using a set of spectral lines of Cr I Cr II Fe I Fe II with different lower level excitation energies. The adapted distributions are shown in Fig. 3. Fe stratification is necessary to correctly account for blends.

Synthetic spectrum calculation in our Cr I line regions was performed following the method described in Sect. 3. The surface magnetic field B_s = 5.4 kG was derived from the

Article published by EDP Sciences and available at http://www.edpsciences.org/aa or http://dx.doi.org/10.1051/0004-6361:20042318

Table 1. continued.

PERTURBERS ARE:		ELECTRONS		PROTONS		HELIUM IONS	
TRANSITION	T(K)	*FWHM*(A)	SHIFT(A)	*FWHM*(A)	SHIFT(A)	*FWHM*(A)	SHIFT(A)
Cr I $^7P^0_3$–$^7D_4$	2500.	0.182E–01	0.452E–03	0.109E–01	–0.737E–02	*0.683E–02	–0.564E–02
	5000.	0.156E–01	0.277E–03	0.130E–01	–0.902E–02	*0.788E–02	–0.664E–02
5297.38 A	10 000.	0.131E–01	0.129E–03	0.144E–01	–0.102E–01	0.909E–02	–0.787E–02
C = 0.12E+15	20 000.	0.108E–01	–0.434E–04	0.168E–01	–0.945E–02	0.956E–02	–0.934E–02
	30 000.	0.956E–02	–0.141E–03	0.172E–01	–0.830E–02	0.945E–02	–0.100E–01
	50 000.	0.822E–02	–0.240E–03	0.194E–01	–0.603E–02	0.793E–02	–0.100E–01
Cr I $^7P^0_4$–$^7D_3$	2500.	0.245E–01	–0.956E–03	*0.220E–01	–0.141E–01	*0.134E-01	–0.104E–01
	5000.	0.214E–01	–0.701E–03	*0.259E–01	–0.173E–01	*0.155E–01	–0.127E–01
5329.78 A	10 000.	0.181E–01	–0.492E–03	*0.280E–01	–0.197E–01	*0.173E–01	–0.153E–01
C = 0.61E+14	20 000.	0.150E–01	–0.419E–03	0.286E–01	–0.197E–01	*0.173E–01	–0.182E–01
	30 000.	0.134E–01	–0.411E–03	0.289E–01	–0.184E–01	*0.160E–01	–0.197E–01
	50 000.	0.115E–01	–0.410E–03	0.295E–01	–0.159E–01	*0.130E–01	–0.204E–01
Cr I $^7P^0_4$–$^7D_4$	2500.	0.184E–01	0.460E–03	0.110E–01	–0.746E–02	*0.692E–02	–0.570E–02
	5000.	0.158E–01	0.276E–03	0.132E–01	–0.911E–02	*0.798E–02	–0.672E–02
5329.14 A	10 000.	0.132E–01	0.127E–03	0.146E–01	–0.103E–01	0.920E–02	–0.796E–02
C = 0.12E+15	20 000.	0.109E–01	–0.484E–04	0.170E–01	–0.956E–02	0.967E–02	–0.946E–02
	30 000.	0.968E–02	–0.147E–03	0.174E–01	–0.840E–02	0.956E–02	–0.101E–01
	50 000.	0.832E–02	–0.248E–03	0.197E–01	–0.610E–02	0.802E–02	–0.101E–01
Cr I $^7P^0_4$–$^7D_5$	2500.	0.920E–02	0.162E–02	0.499E–02	0.407E–02	0.370E–02	0.321E–02
	5000.	0.800E–02	0.979E–03	0.599E–02	0.470E–02	0.417E–02	0.372E–02
5328.32 A	10 000.	0.678E–02	0.474E–03	0.739E–02	0.544E–02	0.473E–02	0.426E–02
C = 0.40E+15	20 000.	0.567E–02	0.103E–03	0.902E–02	0.641E–02	0.543E–02	0.485E–02
	30 000.	0.509E–02	–0.604E–04	0.987E–02	0.709E–02	0.590E–02	0.526E–02
	50 000.	0.445E–02	–0.208E–03	0.106E–01	0.784E–02	0.647E–02	0.589E–02

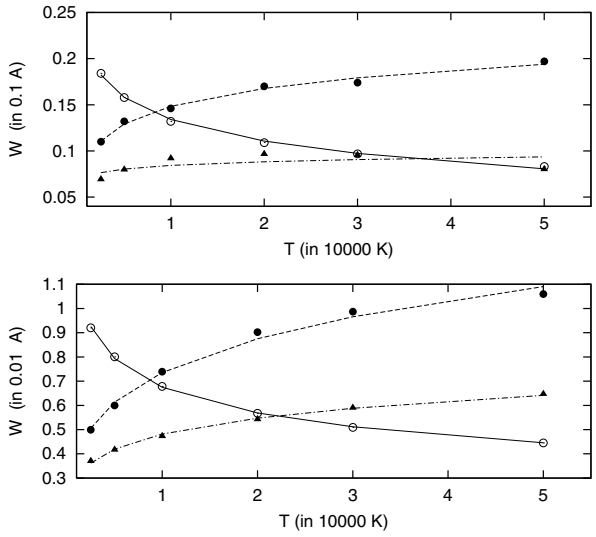

Fig. 1. The analytic fit of Cr I λ = 5329.14 Å (*upper figure*) and λ = 5328.32 Å (*down*) Stark widths due to impact with electrons (open circles), protons (full circles), and He II (full triangles).

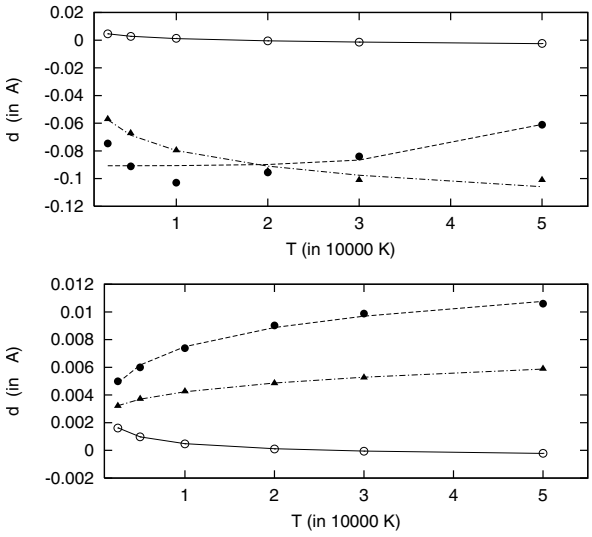

Fig. 2. The same as in Fig. 1, but for Stark shift.

magnetically split lines and used in all calculations. In the calculation process we found that Cr I lines have incorrect wavelengths with shifts up to 0.05 Å. We adjusted wavelengths by calculating the solar synthetic spectrum and comparing it with the Solar Flux Atlas (Kurucz et al. 1984). Improved wavelengths of Cr I lines derived this way agree within 0.005 Å and better with the precise measurements of J. E. Murray (1992), kindly provided to us by R. Kurucz[1]. We placed Murray's

[1] http://cfaku5.cfa.harvard.edu/atoms/2400/

Article published by EDP Sciences and available at http://www.edpsciences.org/aa or http://dx.doi.org/10.1051/0004-6361:20042318

Table 2. The parameters A, B, and C of the approximate formulas for Stark widths and shifts. * - fit with 3 values.

Line	5276.07 Å	5275.75 Å	5275.28 Å	5298.49 Å	5298.02 Å	5297.38 Å	5329.78 Å	5329.14 Å	5328.32 Å
					WIDTH				
					Electrons				
c_1	1E–16	1E–15	1E–15	1E–15	1E–15	1E–15	1E–15	1E–15	1E–16
A	–0.3474	–0.86156	–0.8218	–0.86039	–0.82019	–0.8674	–0.81818	–0.86596	–0.325497
B	–0.15596	–0.03684	–0.04346	–0.03716	–0.04412	–0.0337	–0.04412	–0.03410	–0.161576
					Protons				
c_1	1E–16	1E–15	1E–15	1E–15	1E–15	1E–15	1E–15	1E–15	1E–15
A	–0.3194	–0.23723*	–0.7393	–0.2312*	–0.7368	–0.85357	–0.7338	–0.85169	–0.924767
B	0.1789	–0.06276*	0.02231	–0.062768*	0.02238	0.02723	0.02281	0.027692	0.01959
					He II				
c_1	1E–16	–	1E–15	–	1E–15	1E–16	1E–15	1E–16	1E–16
A	–0.5525	–	–0.84377	–	–0.84219	–0.14236	–0.84037*	–0.13199	–0.51847
B	0.08565	–	0.01192	–	0.011451	0.11010	0.01177*	0.110894	0.092283
					SHIFT				
					Electrons				
c_2	1E–16	1E–16	1E–17	1E–16	1E–17	1E–17	1E–17	1E–17	1E–16
A	–3.4929	–6.7617	–81.5107	–2.5259	–9.0041	49.6736	–16.5511	40.5533	23.3420
B	0.01451	0.00793	0.00221	0.02206	0.02144	0.00526	0.01131	0.00586	0.00261
C	3.3728	6.6362	80.9250	2.3985	8.4079	–49.60704	15.9454	–40.4305	–23.2800
					Protons				
c_2	1E–16	1E–15	1E–15	1E–15	1E–15	1E–16	1E–15	1E–16	1E–16
A	–0.0170	0.25969*	3.0908	–3.3759*	0.5500	–2.4538	3.7646	18.8373	50.1882
B	0.22391	–0.122027*	0.00215	0.00846*	0.00990	0.02228	0.00188	–0.00173	–0.002557
C	–0.4916	–0.6076*	–3.2607	3.0621*	–0.7217	1.6060	–3.9381	–19.6934	–49.62339
					He II				
c_2	1E–16	–	1E–15	–	1E–15	1E–16	1E–15	1E–16	1E–16
A	–0.0174	–	1.7973	–	2.4949	37.4669	2.0440	36.5920	0.0405
B	0.20567	–	0.01778	–	0.01314	0.00418	0.01604	0.00431	0.22021
C	–0.3771	–	–1.9474	–	–2.6462	–38.2561	–2.1971	–37.3904	0.3832

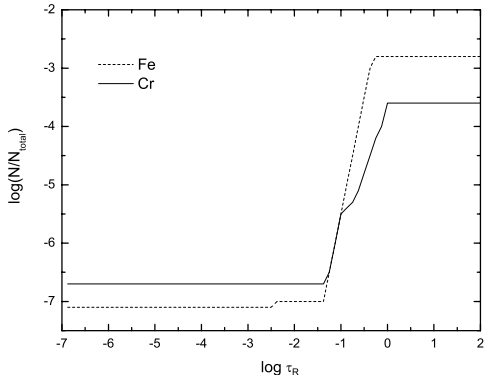

Fig. 3. Empirically derived Cr and Fe distributions in the atmosphere of magnetic Ap star β CrB.

wavelengths in Tables 1 and 2 and used them in spectral synthesis. We also estimated the contribution of Van der Waals broadening and found it to be one order of magnitude smaller than Stark broadening through the whole atmosphere above $\log(\tau_{5000}) = -0.2$ with rapid decrease below the photosphere.

We varied Stark broadening parameters given in Table 1 to achieve a best fit of the calculated Cr I line profiles to observations. Figure 4 shows a comparison between observations and calculations in the region of 3 groups of Cr I lines. For comparison we present synthetic calculations with homogeneous mean abundances $\log(\mathrm{Cr}/N_{\mathrm{tot}}) = -4.80$ and $\log(\mathrm{Fe}/N_{\mathrm{tot}}) = -4.15$, which were used in model atmosphere calculations (Kupka et al. 2004). To fit Cr I line wings we need to decrease current Stark widths by 60–70%. The same order of overestimation of Stark damping constants, was obtained for Si I lines (see Dimitrijević et al. 2003) calculated within the semiclassical perturbation formalism. Any change in Cr distribution, that may be responsible for line profiles, too, is critical for nearby Cr I λ 5296.691 Å, which is insensitive to the Stark broadening mechanism because of the small value of the Stark damping constant and because it is only sensitive to Cr distribution in stellar atmospheres. We also compare observations with a

Article published by EDP Sciences and available at http://www.edpsciences.org/aa or http://dx.doi.org/10.1051/0004-6361:20042318

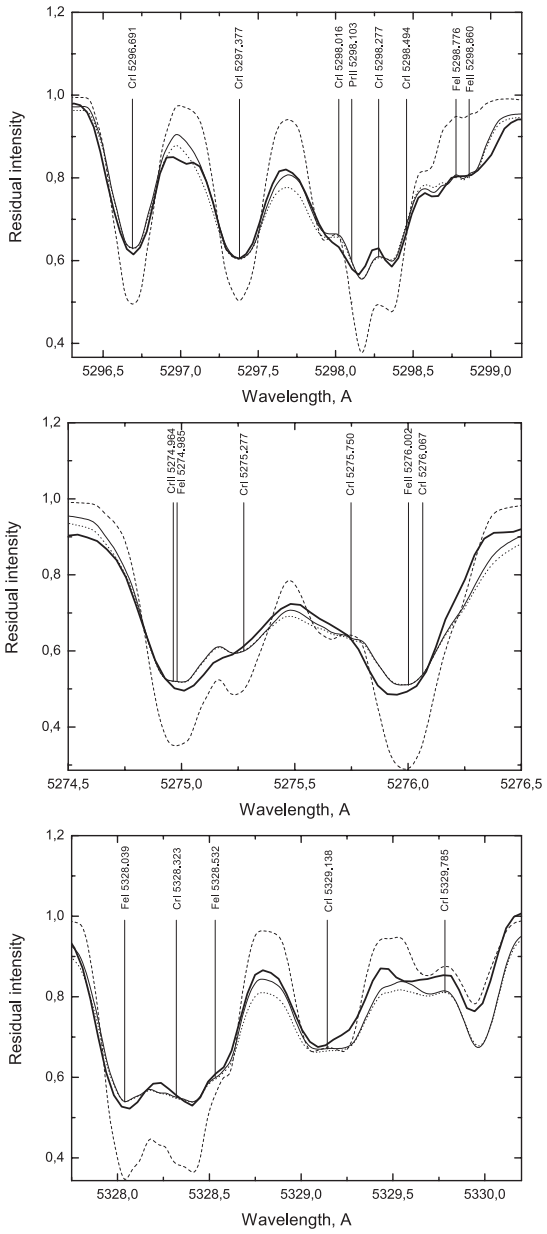

Fig. 4. A comparison between synthetic spectrum calculations and the observed spectrum (thick line) of magnetic Ap star β CrB in the regions of Cr I lines 5297 Å (*top panel*), 5276 Å (*middle panel*), and 5329 Å (*bottom panel*). Full thin line – calculations with stratification shown in Fig. 3 and Stark broadening data from Table 1 decreased by 70%; dashed line – the same Stark broadening data but homogeneous Cr and Fe abundances (see text); dotted line – stratified Cr and Fe abundances, but Stark broadening calculated with the approximation formula.

synthetic spectrum calculated using stratified Cr distribution and an approximation formula for Stark broadening (Cowley 1971). This formula is used in the cases where Stark broadening data, experimental or theoretical, are not available. Evidently, Stark broadening is overestimated when calculations are performed with this approximation formula.

For a more detailed investigation of the influence of Stark shifts on the observed line profile, we calculated theoretical spectra with and without shifts for two separate

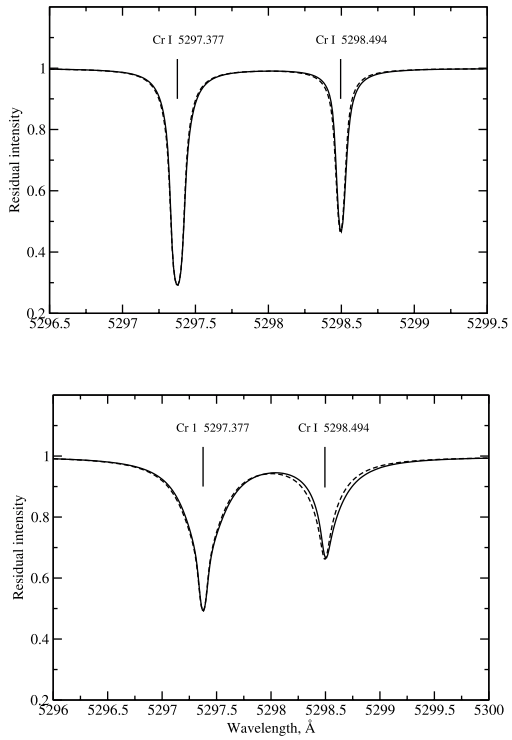

Fig. 5. Influence of Stark shift on Cr I line shapes in homogeneous (*upper panel*) and in stratified (*lower panel*) atmospheres. Calculations with both Stark widths and shifts are shown by solid lines, while those without Stark shifts are shown by a dashed line.

Cr I lines 5297.377 Å and 5298.494 Å in homogeneous and stratified atmospheres of the non-rotating star. These two lines have the smallest and largest shift values, therefore one can make a relative comparison. Figure 5 illustrates the influence of the Stark shift on line shape. The total shift in line position due to the Stark broadening effect is negligible for Cr I 5297.377 Å line both in homogeneous and stratified atmospheres. For the second line, Stark broadening leads to a theoretically measurable shift in the line position, in particular, in the case of Cr stratification resulting in a small line asymmetry. Unfortunately, in spectra of real stars, the effect is difficult to measure due to other broadening mechanisms (rotation, magnetic field) and mainly due to severe blending in the regions with Cr I lines from 4p−4d transitions.

5. Conclusions

Stark broadening parameters for Cr I spectral lines from the $4p^7P^0-4d^7D$ multiplet were calculated and the influence of Stark broadening effect was investigated in stellar atmospheres for these lines. From our investigation we can conclude:

(i) Although they belong to the same multiplet, the widths and shifts of the different lines can be quite different.
(ii) Contribution of the proton and He II collisions to the line width and shift is significant and is comparable and, depending of the electron temperature, even larger than electron-impact contribution.
(iii) Depending on the electron-, proton-, and He II density in stellar atmospheres, the Stark shift may contribute to the

Article published by EDP Sciences and available at http://www.edpsciences.org/aa or http://dx.doi.org/10.1051/0004-6361:20042318

blue, as well as to the red, asymmetry of the same line (see Fig. 2).

(iv) To fit Cr I line wings well we need to decrease the calculated Stark widths by 60−70%, which is the same order of overestimation as for Si I lines (Dimitrijević et al. 2003). Used in the cases where the adequate semiclassical calculation is not possible due to the lack of reliable atomic data, the approximation formula of Cowley (1971) also predicts the overestimated influence of Stark broadening in comparison with observations.

Acknowledgements. We are very thankful to G. Wade and R. Kurucz who provided us with the data necessary for our analysis. This work is a part of the projects GA-1195 "Influence of collisional processes on astrophysical plasma lineshapes" and GA-1196 "Astrophysical Spectroscopy of Extragalactic Objects" supported by the Ministry of Science and Environment protection of Serbia. The research was supported also by the Fonds zur Förderung der wissenschaftlichen Forschung *P14984*. T.R. thanks Leading Scientific School grant 162.2003.02 and the RFBR (grant 03-02-16342) for partial funding. L.Č.P. is supported by Alexander von Humboldt Foundation through the program for foreign scholars. D.S. acknowledges financial support from INTAS grant 03-55-652.

References

Babel, J. 1992, A&A, 258, 449
Bates, D. R., & Damgaard, A. 1949, Trans. Roy. Soc. London, Ser. A, 242, 101
Cowley, C. R. 1971, Obs., 91, 139
Dimitrijević, M. S. 1996, Zh. Priklad. Spektrosk., 63, 810
Dimitrijević, M. S., & Sahal-Bréchot, S. 1984a, JQSRT, 31, 301
Dimitrijević, M. S., & Sahal-Bréchot, S. 1984b, A&A, 136, 289
Dimitrijević, M. S., Ryabchikova, T., Popović, L. Č., Shulyak, D., & Tsymbal, V. 2003, A&A, 404, 1099
Humlicek, J. 1982, JQSRT, 27, 437
Khan, S. 2004, JQSRT, 88, 71
Kupka, F., Piskunov, N. E., Ryabchikova, T. A., Stempels, H. C., & Weiss, W. W. 1999, A&AS, 138, 119
Kupka, F., Paunzen, E., Iliev, I. Kh., & Maitzen, H. M. 2004, MNRAS, 352, 863
Kurucz, R. L. 1993, CDROM13, SAO, Cambridge
Kurucz, R. L., Furenlid, I., Brault, J., & Testerman, L. 1984, NSO Atlas No. 1: Solar Flux Atlas from 296 to 1300 nm, Sunspot, NSO
Moore, C. E. 1971, Atomic Energy Levels Vol. II, NSRDS-NBS 35 (Washington: US Gov. Print. Office)
Murray, J. E. 1992, Ph.D. Thesis, Imperial College, London
Oertel, G. K., & Shomo, L. P. 1968, ApJS, 16, 175
Piskunov, N., & Kupka, F. 2001, ApJ, 547, 1040
Piskunov, N., & Kochukhov, O. 2002, A&A, 381, 736
Popović, L. Č., Dimitrijević, M. S., & Ryabchikova, T. 1999, A&A, 350, 719
Popović, L. Č., Simić, S., Milovanović, N., & Dimitrijević, M. S. 2001, ApJS, 135, 109
Rees, D. E., Murphy, G. A., & Durrant, C. J. 1989, ApJ, 339, 1093
Ryabchikova, T., Piskunov, N., Kochukhov, O., et al. 2002, A&A, 384, 545
Ryabchikova, T., Wade, G., & LeBlanc, F. 2003, in Modelling of Stellar Atmospheres, ed. N. E. Piskunov, W. W. Weiss, & D. F. Gray, ASP, IAU Symp., 210, 301
Sahal-Bréchot, S. 1969a, A&A, 1, 91
Sahal-Bréchot, S. 1969b, A&A, 2, 322
Sahal-Bréchot, S. 1974, A&A, 35, 321
Sobelman, I. I. 1977, Introduction to the theory of atomic spectra (Moscow: Nauka)
Socas-Navarro, H., Trujillo Bueno, J., & Ruiz Cobo, B. 2000, ApJ, 530, 97
van Regemorter, H., Hoang Binh Dy, & Prud'homme, M. 1979, J. Phys. B, 12, 1073
Wade, G. A., Ryabchikova, T. A., Bagnulo, S., & Piskunov, N. 2001, in Magnetic Fields Across the Hertzsprung-Russell Diagram, ed. G. Mathys, S. K. Solanki, & D. T. Wickramasinghe, ASP Conf. Ser., 248, 341
Wade, G. A., LeBlanc, F., Ryabchikova, T. A., & Kudryavtsev, D. 2003, in Modelling of Stellar Atmospheres, ed. N. E. Piskunov, W. W. Weiss, & D. F. Gray, CD-D7, IAU Symp., 210
Wiese, W. L., & Musgrove, A. 1989, Atomic Data for Fusion Vol. 6, Spectroscopic Data for Titanium, Chromium and Nickel, Vol. 2. Chromium, Controled Fusion Atomic Data Center, Oak Ridge National Laboratory, Oak Ridge

Article published by EDP Sciences and available at http://www.edpsciences.org/aa or http://dx.doi.org/10.1051/0004-6361:20042318